Determination of the COSY Proton–Beam Dimensions by means of the COSY–11 Detection System

P. Moskal* for the COSY–11 collaboration

At the COSY–11 facility [1] (see Fig. 1) the production of short-living uncharged mesons, like η, ω, η', or ϕ, is investigated by means of the missing mass technique in the $pp \to ppX$ reaction. The accuracy of the missing mass

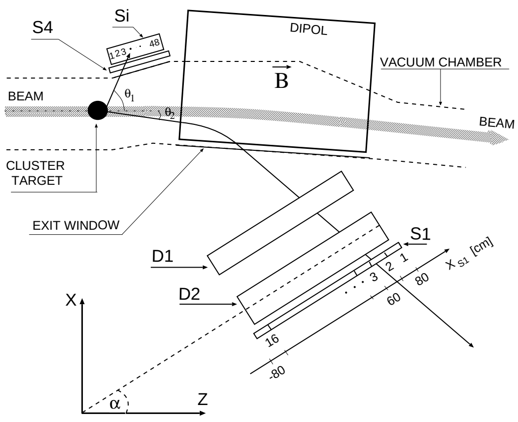

Figure 1: Schematic view of the COSY–11 detection setup. Only detectors used for the measurement of elastically scattered protons are shown. Numbers, at the silicon pad detector (Si) and below the scintillator hodoscope (S1), indicate the order of segments. D1 and D2 denote drift chambers. The X_{S1} axis is defined such that the first segment of the S1 ends at 80 cm and the sixteenth ends at -80 cm.

determination, which decides whether the signal from the given meson is visible over a multi–pion background, depends on the accuracy of the momentum reconstruction of the registered protons, which in turn depends on the detector resolution and the momentum– and geometrical spread of the proton beam. The momentum reconstruction is performed by tracing back trajectories from the drift chambers through the dipole magnetic field to the target, which is assumed to be a vertical line. In reality, however, reactions take place in that region of finite dimensions where beam and target overlap (see Fig. 2). Therefore, assuming in the analysis an infinitesimal target implies a smearing out of the momentum vectors and hence of the missing mass signal. It is not possible to determine the vertex of the reaction on an event–by–event basis and to correct for this effect. However, if the target and beam dimensions were known it would be possible to determine the average smearing of the missing mass originating from this effect and hence to infer the natural width of the measured mesons, provided that the beam momentum spread is known as well. The knowledge of the dimensions and relative settings of beam and target is also crucial for the determination of the acceptance of the detection system.

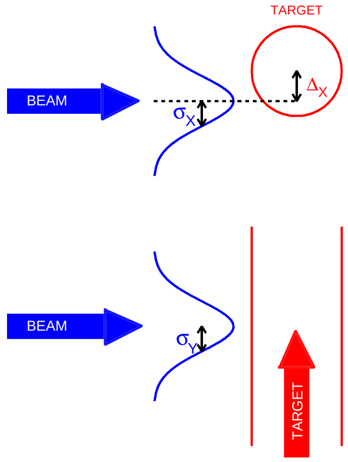

Figure 2: Schematic description of the relative beam and target setting. Seen from above (upper part), and from aside (lower part), σ_X and σ_Y denote the horizontal and vertical standard deviation of the assumed Gaussian distribution of the proton beam density, respectively. The distance between the middle of the proton beam and the target centre is described as Δ_X.

In this report we present a method of estimating the dimensions of the COSY proton beam based on the momentum distribution for elastically scattered protons, which are always measured simultaneously with the investigated reaction. The part of the COSY–11 detection setup used for the registration of elastically scattered protons is shown in Figure 1. The two body kinematics gives an unambiguous relation between the recoil angles Θ_1 and Θ_2 of both scattered protons (see Figure 1). Therefore, as can be seen in Figure 3, the events of elastically scattered protons can be identified from the correlation line formed between the position in the silicon pad detector Si and the scintillator hodoscope S1. For the proton scattered in forward direction and deflected in the magnetic field of the dipole the momentum vector at the target point can be determined. According to two–body kinematics, momentum components parallel and perpendicular to the beam axis should form an ellipse, with a section shown as a solid line in Figure 4, which also presents data selected according to the correlation criterion from Figure 3. The mean of data is clearly shifted from the expected line, reconstructed momenta are on average larger than expected. This observation can not

*Institute of Physics, Jagellonian University, 30–059 Cracow, Poland

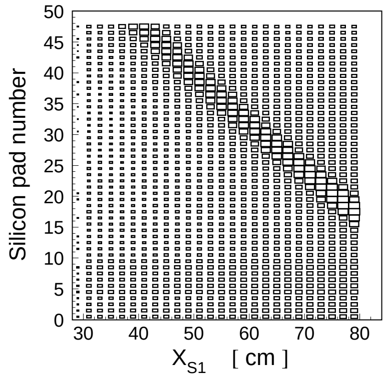

Figure 3: Pad number of the silicon detector Si versus the position in the S1 detector. Note that the number of entries per bin is given in a logarithmic scale.

be explained, neither by a wrong estimation of the proton beam momentum, nor by a wrong assumption of the proton beam angle. In order to correct for this effect the beam momentum must have been changed by more than 120 MeV/c (dashed line in Figure 4), which is 40 times more than the conservatively estimated error of the absolute beam momentum (± 3 MeV/c). Similarly, the effect could have been corrected by changing the beam angle by 40 mrad (see dashed-dotted line), which also exceeds the admissible deviation of the beam angle (± 1 mrad [3]) by at least a factor of 40.

However, the observed discrepancy can be explained by a shift of the assumed reaction point of -0.25 cm in the direction perpendicular to the beam, along the X-axis defined in Figure 1. The momentum components obtained under this assumption, shown in Figure 5, agree with the expectation depicted by the solid line, and the data are now spread symmetrically around the theoretical line. This spread is primarily due to the approximation of a point–like target, and also, but to a much smaller extent, due to multiple scattering and the spread of the beam momentum. The last two effects cause a dispersion in the order of the line thickness.

Assuming the target to be described by a cylindrical pipe homogeneously filled with protons, and the proton beam density distribution by Gaussian functions with standard deviations σ_X and σ_Y for the horizontal and vertical directions, respectively, we performed Monte–Carlo simulations varying Δ_X and σ_X (see Fig. 2). The simulated events were stored and analysed in the same way as the experimental data. The comparison of the data from Figure 4 with the corresponding simulated histograms allowed to determine the horizontal proton beam extension σ_X and the relative shift of target and beam Δ_X. Figure 6 shows the logarithm of the obtained χ^2 as a function of the values of σ_X and Δ_X assumed in the Monte–Carlo calculations: A valley with a minimum is clearly recognizable, which gives the unique possibility to determine the varied parameters σ_X and Δ_X. The minimum of the

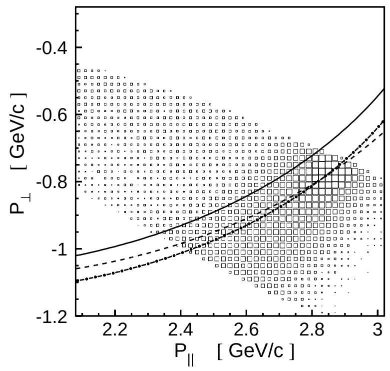

Figure 4: Perpendicular versus parallel momentum components with respect to the beam direction of particles registered at a beam momentum of 3.227 GeV/c. The number of entries per bin is shown logarithmically. The solid line corresponds to the momentum ellipse expected for protons scattered elastically at a beam momentum of 3.227 GeV/c, the dashed line refers to a beam momentum of 3.350 GeV/c, and the dashed-dotted line shows the momentum ellipse obtained for a proton beam inclined by 40 mrad.

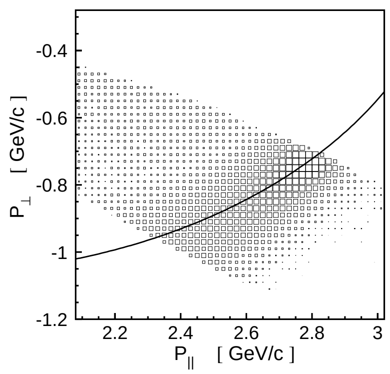

Figure 5: Same data as shown in Figure 4 but analysed with the target point shifted by -0.25 cm perpendicularly to the beam direction (along the X-axis in Figure 1). The solid line shows the momentum ellipse at a beam momentum of 3.227 GeV/c.

χ^2–distribution, at σ_X = 0.15 cm and Δ_X = 0.3 cm, is better seen in Figures 7 and 8, the χ^2 was calculated according to [4]:

$$\chi^2 = \sum_i \left[2(N_i^s - N_i^e) + 2 \cdot N_i^e ln(N_i^e/N_i^s)\right] \qquad (1)$$

where N_i^e and N_i^s denote the content of the i^{th} bin of the $P_\perp$–versus–$P_{||}$ spectrum determined from experiment (Fig. 4) and simulations, respectively.

The vertical beam extension of σ_Y=0.53 cm was established directly from the distribution of the vertical component of the particle trajectories at the centre of the target. This is possible, since for the momentum reconstruc-

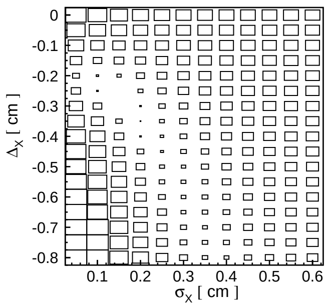

Figure 6: χ^2 as a function of σ_X and Δ_X.

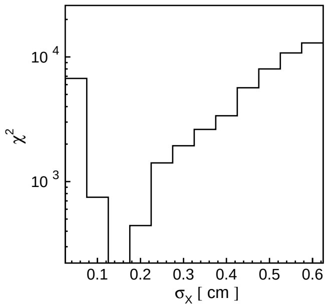

Figure 7: χ^2 as a function of σ_X.

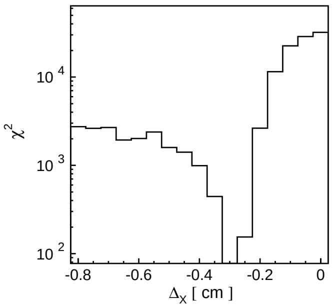

Figure 8: χ^2 as a function of Δ_X.

tion only the origin of the track in the horizontal plane is used, while the vertical component remains a free parameter. As shown in Figure 9, the reconstructed distribution of the vertical component of the reaction points indeed can be well described by a Gaussian distribution.
The effect of a possible drift chamber misalignment, i. e. an inexactness of an angle α in Figure 1, was estimated to cause a shift in the momentum plane corresponding to a value of 0.15 cm for Δ_X. This gives a rather large systematical bias to the estimation of the absolute value of Δ_X, but it does not influence the implications concerning the parameter σ_X. Changes of the beam parameters during the 60 minutes measurement cycle were also neglected. A more detailed analysis studying beam condition changes during the cycle — from heating the beam due to scattering in the target and from stochastically cooling the beam — is in progress. Preliminary results show, that the beam shrinks during the cycle in the horizontal plane, and simultaneously broadens in the vertical one.

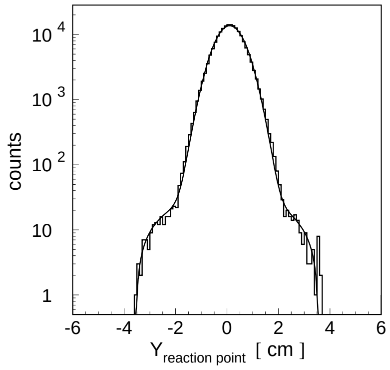

Figure 9: Distribution of the vertical component of the reaction points determined by tracing back trajectories from the drift chambers through the dipole magnetic field to the centre of the target (in the horizontal plane). "Tails" are due to secondary scattering on the vacuum chamber and were parametrized by a polynomial of second order. The solid line shows the simultaneous fit of the Gaussian distribution and the polynomial of second order.

References:

[1] S. Brauksiepe et al., Nucl. Instr. & Meth. A 376 (1996) 397

[2] H. Dombrowski et al., Nucl. Instr. & Meth. A 386 (1997) 228

[3] D. Prasuhn, private communications.

[4] S. Baker, R. Cousins, Nucl. Instr. & Meth. 221 (1984) 437